

SUPERFAST LINE PROFILE VARIATIONS IN THE SPECTRA OF OBA STARS III: A0 STAR α^2 CVn, NEW RESULTS

A. F. Kholtygin,^{1,*} A. V. Moiseeva,² I. A. Yakunin,^{1,2} S. Hubrig³

¹*Saint Petersburg State University, Saint Petersburg, 199034 Russia*

²*Special Astrophysical Observatory, Russian Academy of Sciences, Nizhnii Arkhyz, 369167 Russia*

³*Leibniz-Institut für Astrophysik Potsdam (AIP), Germany*

This work is a continuation of the studies of the ultrafast variability of line profiles in the spectra of early-type stars. Line profile variations (LPVs) in the spectrum a chemically peculiar A0Vp star α^2 CVn are investigated using the January 6, 2020 observations carried out with the 6-meter BTA telescope at Special Astrophysical observatory (SAO) of the Russian Academy of Sciences (RAS) equipped with the MSS spectrograph. Regular short-term periodic variations of the H β , FeII, and Cr II lines were detected with periods ranging from ~ 4 to ~ 140 minutes. The magnetic field of the star was determined for all observations. The average measured longitudinal magnetic field component over the entire duration of observations is about ≈ 600 G, which is close to the value expected from the well-known magnetic field phase curve.

Ключевые слова: stars: variability, pulsations — stars: magnetic field — stars: chemically peculiar — stars: individual: α^2 CVn

1. INTRODUCTION

Although line profile variations in the spectra of OBA stars are well-studied at time scales of hours to days [1–3], the profile variations at minute and second scales remain practically unexplored until now.

The discovery of fast variations in the profiles of lines SiII and FeII in the spectra of an A0 supergiant HD 92207 at time scales of 1–2 minutes by Hubrig et al. [4] prompted us to investigate the superfast spectral variations of early-type stars at minute time scales.

In order of investigate whether the short-term line profile variations in the spectra of OBA-stars are a common phenomenon, we analyzed such variations with a temporal resolution of minutes and fractions of minutes using the SCORPIO low-resolution spectrograph (focal reducer) of the 6-meter telescope of SAO RAS (Afanasiev and Moiseev 2005, [5]), as well as the FORS 2 spectropolarimeter at the 8-meter VLT (Antu) telescope.

A review of observations carried out during the program of looking for the superfast LPVs in the spectra of OBA stars is presented by Batrakov et al. [6] and Tsiopa et al. [7].

Kholtygin et al. [8] presented the results of a study of superfast variations in the spectra of the HD 93521 (O9.5III) star based on the 2015 BTA (SAO RAS) observations. Regular variations with periods of 4–5 and 32–36 minutes were detected. An analysis of the line profiles in the spectrum of Be-star λ Eri obtained with the FORS2 spectropolarimeter by Hubrig et al. [9] showed the presence of variations in the longitudinal magnetic field component with a period of 13.6 minutes. Such variations were also detected in the Balmer and He I line profiles.

Batrakov et al. [6, 10] and Kholtygin et al. [11] presented the results of searching for fast variations in the spectra of the slowly rotating ρ Leo (BIa) supergiant. Regular short period variations of the H and He lines were detected with periods ranging from 2 to 90 minutes. The same star was observed in October–November, 2019 with the 1.25-meter telescope of the Crimean Astronomical Station of Sternberg Astronomical Institute (SAI) of Moscow State University (MSU, [12]). Short-term line profile variations were discovered at times scales of 15–25 minutes.

An analysis of the spectra of the A2 III giant γ UMi obtained in January 2017 with the BTA equipped with the SCORPIO spectrograph showed the presence of harmonic components in the line profile variations with periods in the

* Electronic address: afkholtygin@gmail.com

10–65 minute interval [7].

Of special interest is an investigation of a chemically peculiar and magnetic standard A0Vp star α^2 CVn. Despite the large number of publications¹ dedicated to the study of this star, its short-term variations have practically not been investigated. One may mention only the study by Kuvshinov and Plachinda [13], where the authors investigate variations of the line profiles in the H and K Ca II line center. They report a detection of irregular variations in the profiles of these lines on time scales ranging from minutes to hours.

In a recent paper by Kholtygin et al. [14] authors analyze α^2 CVn observations carried out on January 20/21, 2015 using the BTA telescope equipped with the SCORPIO spectrograph. Short-term regular variations in the Balmer lines and He lines with periods ranging from about \sim 30 to 135 minutes were detected. Using window Fourier transform, we detected quasi-regular transient profile variations in the Balmer lines with 3–6 minute periods.

In this paper we analyze the α^2 CVn BTA observations with a temporal resolution of 2–3 minutes carried out on January 6, 2020. The paper is organized as follows. Section 2 describes the observations and reduction of spectra. Section 3 is dedicated to the variation analysis of the line profiles. Measurements of the stellar magnetic field are presented in Section 4, and a discussion of the obtained results is given in Section 5. Our conclusions are outlined in Section 6.

2. OBSERVATIONS AND REDUCTION OF SPECTRA

The chemically peculiar star α^2 CVn (HD112413) is a magnetic standard. Its effective temperature $T_{\text{eff}} = 11320 \pm 600$ K [15] is higher than that typical for A0 main sequence stars (\sim 9600 K). A rather unusual peculiarity of the α^2 CVn star is the extreme weakness of its X-ray emission. Observations of this star by the Chandra and XMM satellites show that its

X-ray flux $\log L_X < 26.0$ erg/s, which is 3–4 orders of magnitude smaller than the typical values for α^2 CVn-type stars [16].

The radial velocity of α^2 CVn varies significantly on time scales exceeding several months. The radial velocity V_{rad} variations possibly indicate a binarity of α^2 CVn and a presence of a low-mass companion (Romanyuk and Semenko, 2007 [17]). Radial velocity estimates based on SAO RAS observations show that the variation period V_{rad} is probably \approx 60 days or more.

Observations of the star were carried out with the 6-meter BTA telescope within the framework of the “Microvariability in OB stars” program (principal investigator is A.F. Kholtygin, SPbSU) using the MSS spectrograph (Panchuk et al. 2014 [18]) equipped with a circular polarization analyzer (Chountonov et al. [19, 20]) and an image slicer. In order to eliminate the instrumental polarization, circularly polarized spectra were taken in pairs in two phase plate positions changing the polarization plane by 90° . This procedure allows us to consequently obtain an orthogonally polarized signal at the same pixels of the CCD-detector.

In order to control the obtained values, the spectra of magnetic field standards (usually these are stars with a well known magnetic phase curve) and zero polarization standards were obtained.

The primary reduction and spectra extraction were performed with ESO MIDAS system using the ZEEMAN context (Kudryavtsev et al. [21]). The following standard procedures were used for spectra reduction: CCD array bias subtraction, scattered light subtraction, wavelength calibration, after which the one dimensional spectra were normalized to the solar system centroid. When performing wavelength calibration for the series of spectra, we used the nearest in time ThAr lamp spectrum. To normalize the spectra to the continuum, the latter was interpolated by a cubic spline using the "spectool" package in the IRAF² environment. The process of MSS observation reduction is

¹ 1637 ADS citations up to April 22, 2020

² <http://iraf.noao.edu/projects/spectroscopy/spectool/spectool.html>

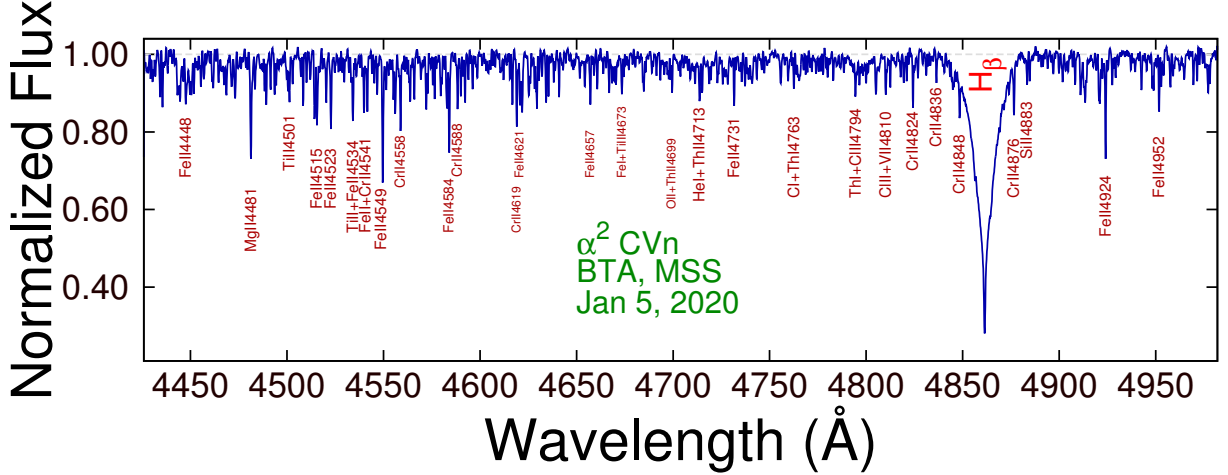


Рис. 1. Average normalized spectrum of α^2 CVn. Marked are the lines investigated for profile variations.

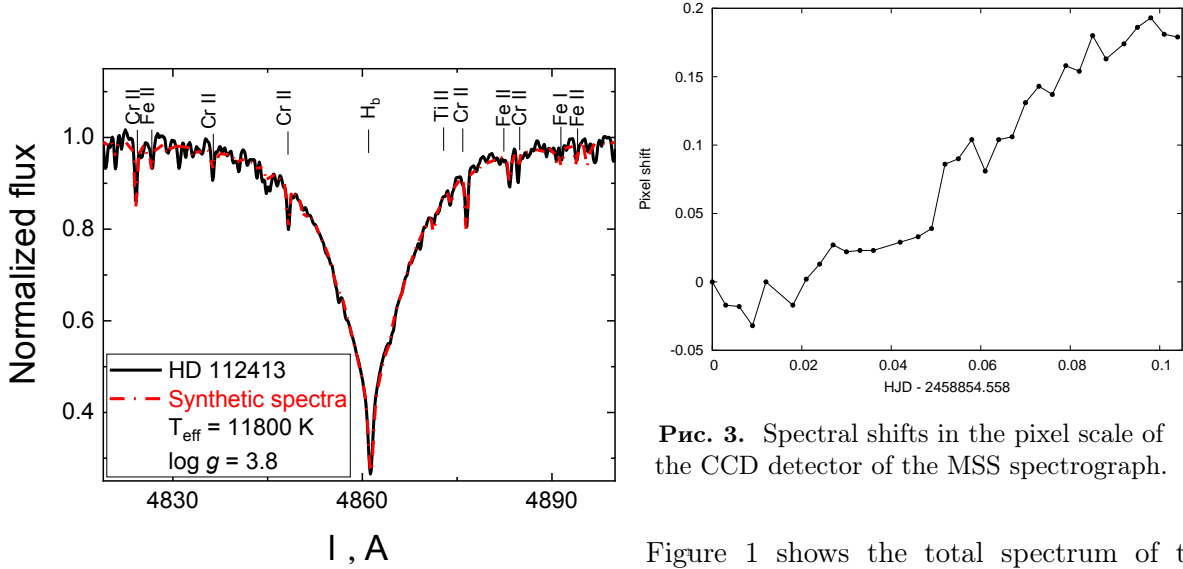


Рис. 2. Synthetic H_β line profile

described in more detail by Kudryavtsev et al. [21] and Semenko et al. [22].

The spectral resolution amounts to about 15000 (slit size $0''.5$), the range of registered wavelengths is 4425–4982 Å, the average S/N is approximately 700. Over the course of our observations with a total time of 156 minutes, we obtained 71 spectra of the star with simultaneously recorded left and right circular polarizations, with an exposure of 90 seconds each. The temporal resolution of one spectrum with account for the CCD detector readout is about 130 seconds.

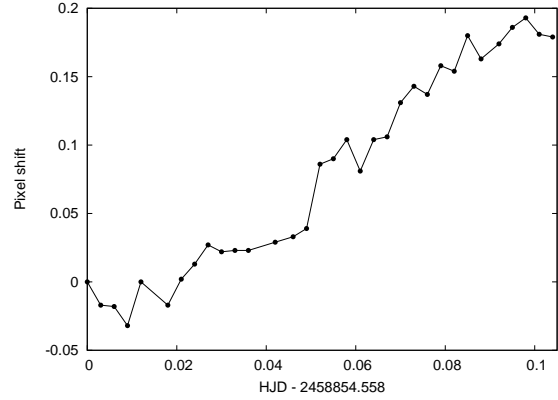


Рис. 3. Spectral shifts in the pixel scale of the CCD detector of the MSS spectrograph.

Figure 1 shows the total spectrum of the star α^2 CVn normalized to the continuum and averaged over all 71 MSS observations:

$$F(\lambda) = F_L(\lambda) + F_R(\lambda), \quad (1)$$

where $F_L(\lambda)$ is the average intensity of the counter clockwise polarized spectral component normalized to the continuum, and $F_R(\lambda)$ is that of the clockwise polarized component.

2.1. Model H_β Line Profile

To refine the parameters of α^2 CVn and determine the radial velocity of the star we model its synthetic spectrum using the ATLAS9 LTE models by Kurucz [23]. The derived synthetic H_β line profile in comparison with the observed

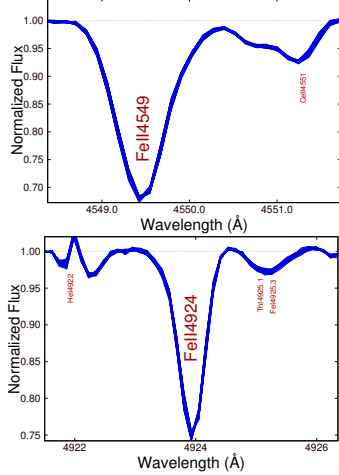


Рис. 4. FeII 4549 (a) and FeII 4924 (b) line profiles for all 71 spectra of α^2 CVn. The variations of individual profiles are small enough to blend into one profile, overlapping each other.

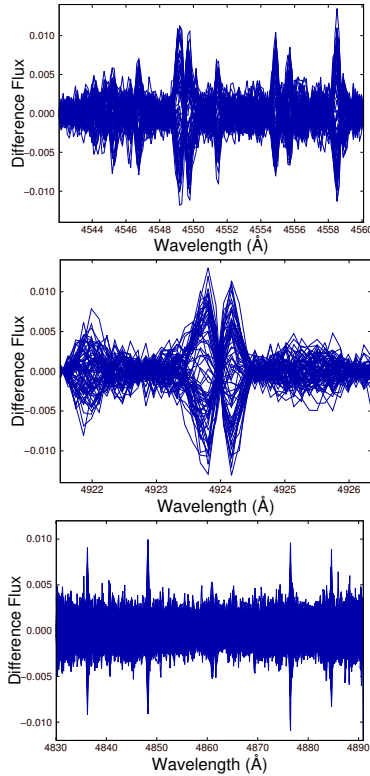


Рис. 5. Deviations of the FeII 4549, FeII 4924, and H_β line profiles from the corresponding average profiles (top to bottom).

profile averaged over all the recorded spectra is presented in Fig. 2. Model parameters were taken

from Kochukhov et al. [24]. For better agreement between the model and observed line profile, the gravity acceleration logarithm $\log g = 4.02$ given by Kochukhov et al. [24] in their Table 3 was reduced to 3.8. Note that the model spectra describes both the H_β and faint CrII 4848.24 and CrII 4876.39731 line profiles with a very high accuracy.

The radial velocities V_{rad} determined by comparing model and observed H_β line profiles from the obtained α^2 CVn spectra are presented in the last column of Table 1.

2.2. Instrumental Effects

When analyzing fast spectral variations one needs to carefully take into account the instrumental errors, which are unavoidable due to the thermal and vibration instability of the spectrograph. The problem of the MSS positional stability has been multiply investigate (see, for example, papers [18, 25, 26]). The pattern of the long-term spectral shift over an interval of about 1.5 days is shown by Panchuk et al. [18]. In addition to the long-term “departures” of the spectrum, rapid variations of its position were also noted. The effects related to the optomechanical instability of the MSS as well as methods of their minimization are described by Klochkova [26]. The results of a study of thermal stability are presented in a SAO preprint by Panchuk et al. [27].

Shifts of 10 microns/hour were detected for the spectral line positions. The typical changes of the position of the spectrum with time in the current MSS configuration includes those a circular polarization analyzer and an image slicer as it presented in Fig. 1 in a paper by Chountonov and Najdenov [25]. As is evident from the figure the drift is linear and does not exceed 0.3 pixels in 2.5 hours. Considering everything mentioned above, the average accuracy of determining the spectral line radial velocities from the MSS spectra is equal to $1.5\text{--}2 \text{ km s}^{-1}$.

To determine the value of the instrumental drift of the spectral lines during the current observation series we performed a cross-

correlation analysis of each consecutive spectrum comparing it with the first one. The results of spectral shift measurements in the pixel scale of the CCD detector are presented in Fig. 3. As is evident from the figure, both a long-term linear drift and short-term variations are present. The total shift between the first and last spectra of the series amounts to 0.18 pixels. Additionally, we used the calibration lamp spectra obtained in the beginning and end of the series, with a difference of 2 hours 40 minutes. Cross-correlation showed a relative shift between two spectra of 0.194 pixels. The detected long-term radial velocity variations are mainly instrumental and were taken into account in further analysis of the α^2 CVn spectra.

3. LINE PROFILE VARIATIONS

When analyzing line profile variations in the spectrum of a star, it is crucial to consider lines of sufficient depth and without significant blending. Based on these principles, we selected 6 lines: MgII 4481, FeII 4549, FeII 4584, CrII 4824, FeII 4924, and H_β .

For illustrative purposes, Fig. 4 shows all the obtained FeII 4549 and FeII 4924 line profiles in the spectrum of α^2 CVn. Their deviations from the average profiles are shown in Fig. 5. As is evident from the figure, the amplitude of the variations does not exceed 1.5%. The changes in the line profiles may be related to the velocity field variations in the atmosphere of the star, for instance, due to non-radial pulsations.

It is noticeable that the amplitude of the H_β line profile variations (Fig. 5, bottom) is significantly smaller than the amplitudes of the FeII 4549 and FeII 4924 line profile variations, as well as those of the narrow lines Fe II and Cr II inside the H_β line profile (see Figs. 1-2). We can assume that such differences are related to the inhomogeneity of the radial distribution of elements (e.g., Silvester et al. [28]).

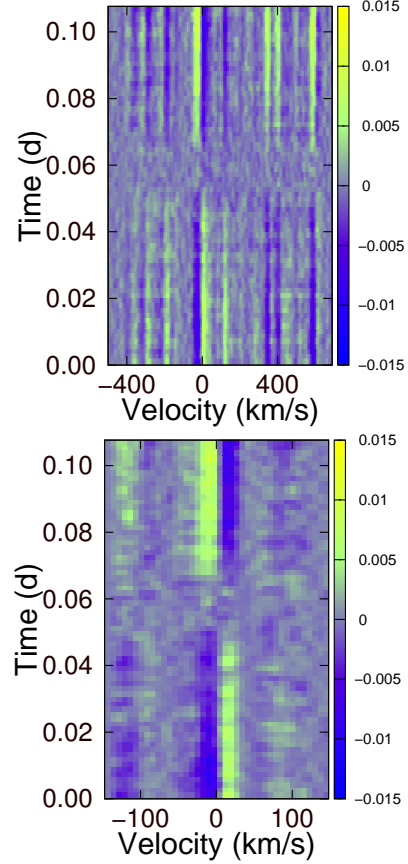


Рис. 6. Dynamic variation spectrum of the FeII 4549 (top) and FeII 4924 (bottom) line profiles.

3.1. Regular Components of the Line Profile Variations

In order to search for the regular components of the profile variations, let us determine the differential line profiles. Let N spectra of the investigated object be obtained as a result of the observations. Let $F_i(\lambda)$, $i = 1, \dots, N$ denotes the continuum normalized flux in the i -th spectrum of the star at the wavelength λ . Let $\overline{F}_i(\lambda)$ be the flux at wavelength λ averaged over all observations. The residual line profile is

$$d(\lambda) = F_i(\lambda) - \overline{F}_i(\lambda) \quad (2)$$

When analyzing subtractive profiles, instead of wavelengths, it is more convenient to use Doppler shifts V from the laboratory wavelength λ_0 of the line $V = c(\lambda/\lambda_0 - 1)$, where c is the speed of light.

If the spectra quality differs significantly, when computing the average and residual line

profiles, one should use different profile weights g_i , proportional to the squared signal-to-noise ratio in the continuum region near the line. However, the signal-to-noise ratios are close in all of our analyzed profiles and we can therefore assume $g_i = 1$.

Figure 6 shows the dynamic variation spectrum for the line profiles of FeII 4549 and FeII 4924 lines in the spectrum of α^2 CVn. Regular changes of the line profiles with time are evident. One can notice that the profile variations are coherent for both FeII 4549 and the neighboring Ti II, Cr II, Fe I and Fe II lines, which indicates a common mechanism of their variations.

We carried out a search for periodic variation components in the line profiles of the α^2 CVn spectrum using the CLEAN method by Roberts et al. [29]. Fourier spectra of the variations of the difference FeII 4549, CrII 4824 and H_β line profiles (periodograms) are presented in Fig. 7 for False Alarm Probability (FAP) value $\alpha = 10^{-3}$.

Regular components exceeding the white noise periodogram counts corresponding to the selected FAP value are presented in the Fourier spectrum. Table 1 gives the detected frequencies and periods of the possible harmonic components of the variations for the analyzed line profiles for $\alpha = 10^{-2} - 10^{-5}$.

For an upper estimation of the Fourier spectrum regular component frequency error we used the expression $\Delta\nu < 1/T$ [30] where $T = 156$ minutes is the total duration of observations. Fourier components with a frequency difference less than $\Delta\nu$ were considered as one component with a frequency corresponding to the average frequency of these components.

The + sign in Table 1 indicates that the corresponding component is present in the Fourier spectrum, and the - sign shows that it has not been detected at the given FAP, although it may be registered at a higher one.

In order to exclude the components corresponding to random outliers of the periodogram, Table 1 includes only the Fourier spectrum components detected in the profile variations of at least two lines.

In the next to last column of the table we present the frequencies of the regular

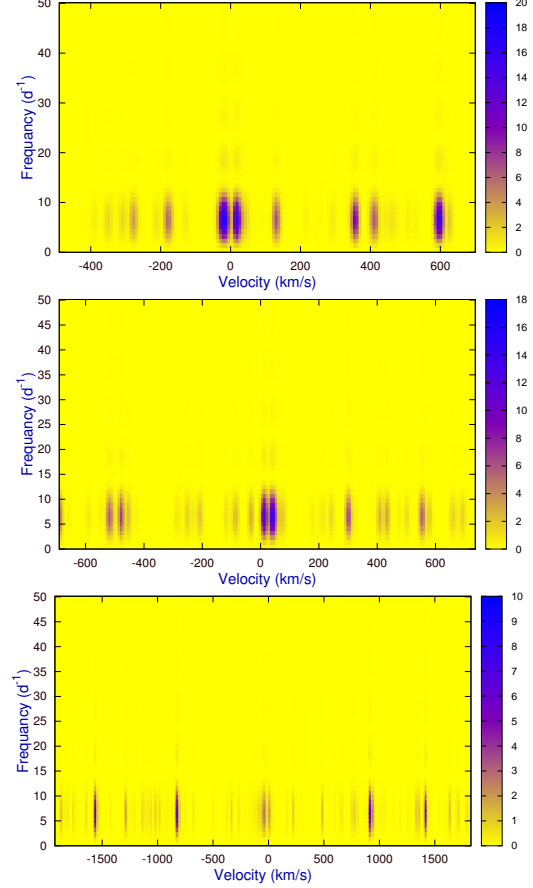


Рис. 7. Fourier spectra of the FeII 4549, CrII 4824 and H_β line profile variations (top to bottom).

components of the profile variations in the spectrum of α^2 CVn obtained from SAO RAS BTA observations in 2015 with the SCORPIO spectrograph (Kholtygin et al. [14]). The corresponding FAP values are given for all of the found components in the last column of the table.

Components $\nu_1 - \nu_4$ correspond to the periods P which exceed the total duration of observations, $T = 156$ minutes. Further observations are needed to verify their reality. Regular line profile variations in the spectra of OB stars with periods close to the periods of components $\nu_1 - \nu_4$ with $P = 3 - 6^h$ are most likely related to non-radial pulsations of the star in quadrupole ($l = 2$) or higher pulsation modes accordingly by Pamyatnykh [31]. The detection of line profile variations in the short period region $P = 15 - 140^m$ may indicate a presence of high mode of non-radial pulsations with $l = 6 - 12$.

Таблица 1. Frequencies (in d^{-1} column 2) and periods (in minutes, column 3) of the regular profile variation components in the spectrum of $\alpha^2\text{CVn}$. The + sign in columns 4–9 indicates that the component was detected in the line profile variations, and the – sign shows that it was not. Column 10 gives the periods of profile variations reported in Kholtygin et al. (2020) [14]. The last column shows FAP values for the detected Fourier components. Components 1–4 have periods longer than the total time of observations.

№	ν (d^{-1})	P (мин)	Mg II 4481	Fe II 4549	Fe II 4584	Cr II 4824	H β	Fe II 4924	[14]	α
1	5.57 ± 9.23	259 ± 429	+	+	+	+	+	+	–	10^{-5}
2	6.50 ± 9.23	222 ± 315	+	+	+	+	+	+	–	10^{-5}
3	7.42 ± 9.23	194 ± 241	+	+	+	+	+	+	–	10^{-5}
4	8.35 ± 9.23	172 ± 190	+	–	–	+	+	–	–	10^{-5}
5	10.67 ± 9.23	135 ± 116	–	+	–	–	+	–	135 ± 164	10^{-2}
6	15.31 ± 9.23	94.0 ± 56.7	+	+	–	–	–	–	–	10^{-2}
7	26.91 ± 9.23	53.5 ± 18.3	+	+	–	–	+	–	52 ± 25	10^{-2}
8	86.31 ± 9.23	16.7 ± 1.8	–	–	–	–	+	+	17.7 ± 2.8	10^{-2}
9	111.37 ± 9.23	12.9 ± 1.1	–	–	+	+	+	–	–	10^{-2}
10	288.64 ± 9.23	4.99 ± 0.16	+	–	+	–	–	–	$4.5\text{--}5.6$	10^{-2}

Three regular profile variation components ν_5 , ν_7 , and ν_8 in the $\nu > 10 \text{d}^{-1}$ frequency region correspond to (with account for errors) the components 135 ± 164 minutes, 52 ± 25 minutes, and 17.7 ± 2.8 minutes reported by Kholtygin et al. [14] which confirms that they are real.

Using the windowed Fourier transform by Kholtygin et al. [14] showed the presence in the LPVs in the spectrum of $\alpha^2\text{CVn}$ of short-period regular components with variable frequency in the 4.5–5.6 minute period interval. The detected by us component ν_{10} corresponds to this frequency interval.

Earlier we interpreted the presence of line profile variation components with such short periods in the spectrum of HD 93521 as evidence for the presence of high modes of non-radial pulsations with $l = 20\text{--}60$ (see Kholtygin et al. [8]). The same interpretation is possible for short-term LPVs in the spectrum of $\alpha^2\text{CVn}$.

4. MAGNETIC FIELD OF $\alpha^2\text{CVN}$

All $\alpha^2\text{CVn}$ spectra were obtained using a circular polarization analyzer, which allows us to estimate the magnetic field of the star. To increase the accuracy of the determined Stokes parameter V we used consecutive observations with different angles of the quarter wave plate:

$$\frac{V}{I} = \frac{1}{2} \left\{ \left(\frac{I^o - I^e}{I^o + I^e} \right)_{-45^\circ} - \left(\frac{I^o - I^e}{I^o + I^e} \right)_{+45^\circ} \right\}, \quad (3)$$

where I^o and I^e are the ordinary and extraordinary beams, correspondingly.

To determine the magnitude of the longitudinal component of the magnetic field averaged over the whole stellar disk (the effective magnetic field, B_e), we used two methods: (1) a modified Babcock method based on measuring shifts of the centers of gravity (cog) of the circularly polarized line components (e.g., Borra and Landstreet [32]), and (2) a regression method based on studying the circular polarization of spectral lines (e.g. Hubrig et al. [4]) using the standard relation:

$$\frac{V}{I} = -\frac{g_{\text{eff}}e}{4\pi m_e c^2} \lambda^2 \frac{1}{I} \frac{dI}{d\lambda} B_e. \quad (4)$$

where g_{eff} is the effective Lande factor of a line, λ is its wavelength, e is the electron charge, and m_e is the electron mass. I is the unpolarized line intensity, $dI/d\lambda$ is the wavelength derivative of Stokes I parameter.

The values of B_e obtained by the cog (B_e^{cog}) and regression (B_e^{reg}) methods and the corresponding standard deviations are presented in Table 2.

Таблица 2. Results of magnetic field and radial velocity measurements for α^2 CVn.

MJD	Phase $P=5.49800$	Phase $P=5.46939$	Phase $P=5.43730$	B_e^{cog} , G	B_e^{egr} , G	V_{rad} , km s^{-1}
58854.058	0.7308	0.8219	0.8850	-662 ± 29	-628 ± 11	-0.31 ± 2.00
58854.061	0.7314	0.8225	0.8855	-752 ± 30	-682 ± 10	-0.24 ± 1.90
58854.064	0.7319	0.8230	0.8861	-677 ± 32	-621 ± 11	-0.39 ± 1.90
58854.067	0.7324	0.8236	0.8866	-624 ± 31	-558 ± 11	-0.36 ± 2.10
58854.070	0.7330	0.8241	0.8872	-732 ± 33	-659 ± 10	-0.12 ± 1.80
58854.076	0.7341	0.8252	0.8883	-676 ± 40	-647 ± 11	-0.30 ± 1.90
58854.079	0.7346	0.8258	0.8888	-684 ± 38	-599 ± 13	-0.09 ± 2.10
58854.082	0.7352	0.8263	0.8894	-643 ± 31	-595 ± 11	-0.09 ± 2.00
58854.085	0.7357	0.8269	0.8899	-616 ± 30	-574 ± 10	-0.01 ± 2.00
58854.088	0.7363	0.8274	0.8905	-679 ± 28	-625 ± 10	-0.04 ± 1.90
58854.091	0.7368	0.8280	0.8910	-679 ± 26	-635 ± 10	0.06 ± 1.80
58854.094	0.7374	0.8285	0.8916	-766 ± 35	-667 ± 10	0.08 ± 1.90
58854.100	0.7385	0.8296	0.8927	-693 ± 28	-660 ± 10	-0.02 ± 2.10
58854.104	0.7392	0.8303	0.8932	-680 ± 29	-618 ± 10	0.09 ± 2.00
58854.107	0.7397	0.8309	0.8938	-732 ± 33	-627 ± 10	0.21 ± 2.00
58854.110	0.7403	0.8314	0.8943	-659 ± 31	-586 ± 11	0.28 ± 1.90
58854.113	0.7408	0.8320	0.8949	-638 ± 32	-579 ± 11	0.33 ± 1.80
58854.116	0.7414	0.8325	0.8954	-605 ± 30	-540 ± 10	0.46 ± 1.90
58854.119	0.7419	0.8331	0.8960	-647 ± 33	-574 ± 10	0.30 ± 2.10
58854.122	0.7425	0.8336	0.8965	-711 ± 41	-654 ± 11	0.47 ± 2.00
58854.125	0.7430	0.8342	0.8971	-785 ± 33	-699 ± 12	0.57 ± 2.00
58854.128	0.7435	0.8347	0.8976	-728 ± 36	-637 ± 12	0.74 ± 1.90
58854.131	0.7441	0.8353	0.8982	-672 ± 36	-568 ± 11	0.84 ± 1.80
58854.134	0.7446	0.8358	0.8988	-603 ± 34	-585 ± 11	0.69 ± 1.90
58854.137	0.7452	0.8364	0.8993	-705 ± 34	-622 ± 11	0.87 ± 2.10
58854.140	0.7457	0.8369	0.8999	-701 ± 33	-635 ± 12	0.83 ± 2.00
58854.143	0.7463	0.8375	0.9004	-674 ± 32	-594 ± 12	1.01 ± 2.00
58854.146	0.7468	0.8380	0.9010	-757 ± 30	-653 ± 11	0.76 ± 1.90
58854.150	0.7475	0.8388	0.9019	-731 ± 34	-655 ± 11	0.91 ± 1.80
58854.153	0.7481	0.8393	0.9024	-702 ± 31	-632 ± 12	0.89 ± 1.90
58854.156	0.7486	0.8399	0.9030	-740 ± 28	-698 ± 11	0.94 ± 2.10
58854.159	0.7492	0.8404	0.9035	-728 ± 30	-679 ± 11	0.91 ± 2.00
58854.162	0.7497	0.8409	0.9041	-769 ± 33	-700 ± 13	0.82 ± 2.00

5. DISCUSSION OF RESULTS

5.1. Influence of Instrumental Effects and Atmospheric Variations on the Line Profile Variations

A rather important question is to what extent the regular profile variation components found in the spectrum of α^2 CVn may be related to instrumental effects and, in particular, to the oscillations of the telescope itself and the detector. An analysis of a large sample of the 6-m SAO RAS telescope observations has shown that the oscillations of the telescope itself are most likely irregular and occur on time

scales uncorrelated with the detected periods (the detailed description of the BTA positional instability are given, for example, Klochkova et al. [26]. With regard to the instrumental drift of the spectral lines discussed in section 2.2, the radial velocity variation analysis presented in Fig. 3 has shown that after the subtraction of the trend in V_{rad} , marginal (FAP level $\alpha > 0.01$) period of about 100 minutes is present, which does not correspond to any of the periods given in Table 1.

Note also that the coincidence of the detected line profile variation periods in the spectrum of α^2 CVn with those derived by Kholtygin et al. [14] using the SCORPIO spectrograph

with another set of intrinsic oscillations also indicates that these periods are real. The set of frequencies and profile variation periods obtained in the analysis of the line profiles of various OBA stars (see references in the introduction) differs significantly, which shows an absence of a connection between the profile variation periods derived in this work and the specific features of the instruments used.

We should also note that some contribution to the line profile variations in the spectrum of the star may be attributed to sporadic variations of the size of the turbulent disk of the star due to atmospheric fluctuations. It is difficult to expect however, that the line profile variations caused by the influence of atmospheric fluctuations would be in any way regular. At the same time, the influence of such fluctuations on the irregular profile variations cannot be ruled out entirely, which should be taken into account during analysis. Additionally, this effect is minimized when using an image slicer, as we did in this case.

5.2. Rotation Period of α^2 CVn and the Magnetic Field Phase Curve

The rotation period of α^2 CVn has been determined as far back as by Farnsworth [33], $P = 5.46939$ d. Consequent studies have slightly refined the period. According to Sikora et al. [34] $P = 5.46913$ d. Recently 27-day photometric observations of α^2 CVn by the TESS satellite have become available [35].

An analysis of these data by the CLEAN method gives $P = 5.43730 \pm 0.470$ d, which corresponds to the values obtained by other authors. To refine the period one must analyze longer series of observations. Due to some uncertainty in the determination of the rotation period of α^2 CVn we varied the period within the limits of its error.

Columns 3–5 in Table 2 show the rotation phases of α^2 CVn for rotation periods $P = 5.46939$ d, $P = 5.49800$ d, and $P = 5.43730$ d. The results of our analysis show that the period of $P = 5.43730$ d derived from an analysis of TESS satellite observations allows us to describe better the dependence of the effective magnetic

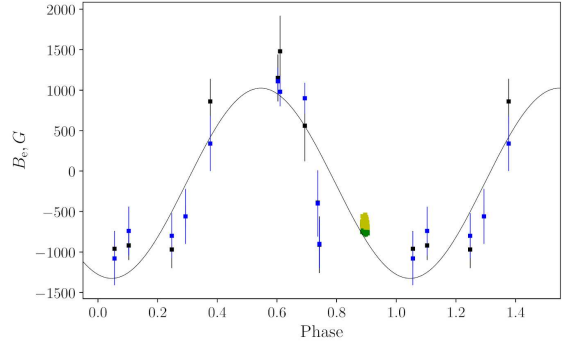


Fig. 8. Phase curve of the effective magnetic field B_e of α^2 CVn with phases corresponding to the rotation period $P = 5.43730$ d. The values of B_e obtained in this work are shown by green (cog method) and yellow (regression method) dots.

field B_e on the rotation phase of the star (phase curve).

The phase curve for $P = 5.43730$ d is shown in Fig. 8. The values of B_e taken from Gerth et al. [36] and Romanyuk et al. [37, 38], are supplemented by values derived in the present work. The determined longitudinal magnetic field values show a good fit with the phase curve. The average of all the measured longitudinal magnetic field values is $B_e = 600 \pm 56$ G.

6. CONCLUSIONS

In this work we studied the line profile variations in the spectrum of the α^2 CVn star with a 2–3 minute temporal resolution based on spectropolarimetric BTA observations with the MSS spectrograph. Regular profile variation components were discovered with periods of 5–140 minutes. The presence of longer regular components is also possible.

We determined the rotation period of α^2 CVn using the TESS satellite photometric data, $P = 5.43730 \pm 0.470$ d. The measured magnetic field corresponds to the magnetic field phase curve for α^2 CVn.

БЛАГОДАРНОСТИ

The authors are grateful to I.I. Romanyuk for advices and recommendations which helped to improve the text of the paper.

FUNDING

A.K. and A.M. acknowledge the support of the RFBR grant 19-02-00311 A. I.Ya. is grateful for the support of this work by the RFBR

project no. 19-32-60007. Observations with the SAO RAS telescopes are carried out with the support of the Ministry of Science and Higher Education of the Russian Federation (including agreement no. 05.619.21.0016, unique project identifier RFMEFI61919X0016).

CONFLICT OF INTEREST

The authors declare no conflict of interest.

-
1. L. Kaper, H. F. Henrichs, A. W. Fullerton, et al., *Astron. and Astrophys.* **327**, 281 (1997).
 2. A. F. Kholtygin, D. N. Monin, A. E. Surkov, and S. N. Fabrika, *Astronomy Letters* **29**, 175 (2003).
 3. V. V. Dushin, A. F. Kholtygin, G. A. Chuntunov, and D. O. Kudryavtsev, *Astrophysical Bulletin* **68**, 184 (2013).
 4. S. Hubrig, M. Schöller, and A. F. Kholtygin, *Monthly Notices Royal Astron. Soc.* **440**, 1779 (2014).
 5. V. L. Afanasiev and A. V. Moiseev, *Astronomy Letters* **31**, 194 (2005).
 6. A. A. Batrakov, A. F. Kholtygin, S. Hubrig, et al., in *Stars and their Variability Observed from Space*, Edited by C. Neiner, W. W. Weiss, D. Baade, et al. (2020), pp. 163–164.
 7. O. Tsiopa, A. Batrakov, A. Kholtygin, et al., *Astronomical Journal of Azerbaijan* **14**, in press (2020).
 8. A. F. Kholtygin, S. Hubrig, V. V. Dushin, et al., in *Stars: From Collapse to Collapse*, Edited by Y. Y. Balega, D. O. Kudryavtsev, I. I. Romanyuk, and I. A. Yakunin (2017), *Astronomical Society of the Pacific Conference Series*, vol. 510, p. 299.
 9. S. Hubrig, I. Ilyin, A. F. Kholtygin, et al., *Astronomische Nachrichten* **338**, 926 (2017).
 10. A. A. Batrakov, A. F. Kholtygin, S. Fabrika, and A. Valeev, in *Physics of Magnetic Stars*, Edited by D. O. Kudryavtsev, I. I. Romanyuk, and I. A. Yakunin (2019), *Astronomical Society of the Pacific Conference Series*, vol. 518, p. 153.
 11. A. F. Kholtygin, A. A. Batrakov, S. N. Fabrika, et al., *Astrophysical Bulletin* **73**, 471 (2018).
 12. A. F. Kholtygin, N. P. Ikonnikova, A. V. Dodin, and O. A. Tsiopa, *Astronomy Letters* **46**, 168 (2020).
 13. V. M. Kuvshinov and S. I. Plachinda, *Bulletin Crimean Astrophysical Observatory* **66**, 144 (1983).
 14. A. F. Kholtygin, A. A. Batrakov, S. N. Fabrika, et al., *Astrophysical Bulletin* **75**, 278 (2020).
 15. J. Sikora, G. A. Wade, J. Power, and C. Neiner, *Monthly Notices Royal Astron. Soc.* **483**, 2300 (2019).
 16. J. Robrade and J. H. M. M. Schmitt, *Astron. and Astrophys.* **531**, A58 (2011).
 17. I. I. Romanyuk and E. A. Semenko, in *Physics of Magnetic Stars*, Edited by I. I. Romanyuk, D. O. Kudryavtsev, O. M. Neizvestnaya, and V. M. Shapoval (2007), pp. 32–60.
 18. V. E. Panchuk, G. A. Chuntunov, and I. D. Naidenov, *Astrophysical Bulletin* **69**, 339 (2014).
 19. G. A. Chountunov, in *Spectroscopic methods in modern astrophysics*, Edited by L. Mashonkina and M. Sachkov (2007), pp. 336–349.
 20. G. A. Chountunov, *Astrophysical Bulletin* **71**, 489 (2016).
 21. D. O. Kudryavtsev, in *Magnetic Fields of Chemically Peculiar and Related Stars*, Edited by Y. V. Glagolevskij and I. I. Romanyuk (2000), pp. 84–88.
 22. E. A. Semenko, I. I. Romanyuk, E. S. Semenova, et al., *Astrophysical Bulletin* **72**, 384 (2017).
 23. R. L. Kurucz, in *IAU Colloq. 138: Peculiar versus Normal Phenomena in A-type and Related Stars*, Edited by M. M. Dworetzky, F. Castelli, and R. Faraggiana (1993), *Astronomical Society of the Pacific Conference Series*, vol. 44, p. 87.
 24. O. Kochukhov, N. Piskunov, I. Ilyin, et al., *Astron. and Astrophys.* **389**, 420 (2002).
 25. G. A. Chountunov and I. D. Najdenov, *Astrophysical Bulletin* **64**, 106 (2009).
 26. V. G. Klochkova, V. E. Panchuk, M. V. Yushkin, and D. S. Nasonov, *Astrophysical Bulletin* **63**, 386 (2008).
 27. V. E. Panchuk, M. V. Yushkin, and E. V. Emelyanov, Preprint SAO, No. 112 p. 11pp

- (2012).
28. J. Silvester, O. Kochukhov, and G. A. Wade, *Monthly Notices Royal Astron. Soc.* **444**, 1442 (2014).
 29. D. H. Roberts, J. Lehar, and J. W. Dreher, *Astron. J.* **93**, 968 (1987).
 30. V. V. Vityazev, SPbSU Press, St. Petersburg, 2001 p. 70 pp. (2001).
 31. A. A. Pamyatnykh, *Acta Astronomica* **49**, 119 (1999).
 32. E. F. Borra and J. D. Landstreet, *Astrophys. J.* **185**, L139 (1973).
 33. G. Farnsworth, *Astrophys. J.* **76**, 313 (1932).
 34. J. Sikora, G. A. Wade, J. Power, and C. Neiner, *Monthly Notices Royal Astron. Soc.* **483**, 3127 (2019).
 35. J. M. Jenkins, J. D. Twicken, S. McCauliff, et al., in *Software and Cyberinfrastructure for Astronomy IV*, Edited by G. Chiozzi and J. C. Guzman (2016), *Society of Photo-Optical Instrumentation Engineers (SPIE) Conference Series*, vol. 9913, p. 99133E.
 36. E. Gerth, Y. V. Glagolevskij, G. Hildebrandt, et al., *Astron. and Astrophys.* **351**, 133 (1999).
 37. I. I. Romanyuk, E. A. Semenko, D. O. Kudryavtsev, and A. V. Moiseeva, *Astrophysical Bulletin* **71**, 302 (2016).
 38. I. I. Romanyuk, E. A. Semenko, A. V. Moiseeva, et al., *Astrophysical Bulletin* **73**, 178 (2018).